Electronic Supplementary Material (ESI) for Green Chemistry.

Supporting Information for: Antioxidant-Induced Transformations of a Metal-Acid Hydrocracking Catalyst in the Deconstruction of Polyethylene Waste

Zachary R. Hinton[1,*], Pavel A. Kots[1,*], Mya Soukaseum[1,2], Brandon C. Vance[1,2], Dionisios G. Vlachos[1,2], Thomas H. Epps, III[1,2,3,†], LaShanda T. J. Korley[1,2,3,†]

[1]Center for Plastics Innovation, University of Delaware, Newark, DE 19716
[2]Department of Chemical and Biomolecular Engineering, University of Delaware, Newark, DE 19716
[3]Department of Materials Science and Engineering, University of Delaware, Newark, DE 19716
*These authors contributed equally
†Corresponding authors

Experimental section

Materials

High-density polyethylene (HDPE) was obtained from Sigma Aldrich (weight-average molecular weight, M_w, ~100 kg/mol, SKU: 427985). Butylated hydroxytoluene (BHT, > 99%, also known as 2,6-di-tert-butyl-4-methylphenol) and pentaerythritol tetrakis(3,5-di-tert-butyl-4-hydroxyhydrocinnamate) (I-1010, 98%) were purchased from Sigma Aldrich. 1,3,5-Tris(3,5-di-tert-butyl-4-hydroxybenzyl)-1,3,5-triazinane-2,4,6-trione (I-3114, >98%) and *n*-octacosane were acquired from TCI America. Xylenes (histological grade) were sourced from Sigma Aldrich. Methanol (Optima® grade), toluene (ACS grade), chloroform (HPLC grade), dichloromethane (DCM, ACS grade), and 1,2,4-trichlorobenzene (HPLC grade) were obtained from Fisher Scientific. All chemicals were used as received.

Extraction and analysis of HDPE additives

Dissolution and recrystallization were preformed to generate an HDPE powder with minimal degradation of polymer chains. As-received HDPE pellets were dissolved (with stirring) in xylenes at 130 °C such that the solution contained 6 wt% polymer. Once fully dissolved (after ~2 h), the solution was cooled slowly (over a period of 30 min) to 60 °C without stirring, at which point a quantity of ice-cold methanol 0.133 times the volume of the solution was slowly added via an addition funnel, and the stirring was restarted. The mixture was then poured into a volume of cold methanol equal to 0.76 times its volume. The recrystallized powder was filtered by vacuum filtration (Fisherbrand P4, 4 µm) and rinsed, first with the filtrate and then once with 200 mL of fresh, room-temperature methanol. The powder was dried in a fume hood for at least 48 h.

Further extraction of additives from the HDPE powder was achieved using Soxhlet extraction. Approximately 8 g of dry, recrystallized HDPE powder was loosely packed into a washed cellulose extraction thimble and placed in the body of a Soxhlet apparatus. 200 mL of chloroform was heated in the flask to boiling, and the temperature setpoint of the hotplate was used to regulate the reflux cycle speed of the extractor until one cycle was completed every ~10 min. The extraction continued for 24 h after completion of the first cycle. The ‘stripped’ polymer was dried

at 60 °C under vacuum for 18 h. This process was repeated in batches to obtain enough material for further experiments.

The extracts from the recrystallization and Soxhlet processes were concentrated using a rotary evaporator. The liquid extracts were separated from the solids formed during cooling by decanting and syringe filtration. Each filtered solution was separately evaporated dry before reconstituting in fresh chloroform at a concentrated volume ratio (chosen to match analyte concentration in the final sample) of 5:3 for recrystallization and 38:1 for Soxhlet extraction. Analysis of the extracts was performed using a gas chromatograph (GC) with dual detectors: a mass spectrometer (MS) and a flame ionization detector (FID) (Shimadzu GC-2030 with GCMS-QP2020 NX) using a fused silica column (Shimadzu SH-I-5MS). The GC program was as follows. Samples were injected with a split ratio of 5:1, with the split temperature maintained at 315 °C. The column was first maintained at 40 °C for 2 min, ramped to 150 °C at 10 °C/min, ramped to 320 °C at 5 °C/min, then maintained at 320 °C for 20 min. The MS ion source temperature was kept at 240 °C, and the full range of mass-to-charge ratio (between 30 and 1090 m/z) was monitored.

Analysis of extracted products was conducted as follows. Retention times for alkanes were calibrated using a known mixture in the range of C_6 – C_{36}. Qualitative identification of compounds was achieved using peaks found in the GC-MS chromatogram. Mass spectra were compared against standards from the National Institute of Standards and Technology (NIST) 2017 Mass Spectral Library. Strict quantification was not achieved because of the complexity in calibrating response factors and accounting for material losses during processing; however, the concentrations of the antioxidants were on the order of 1 wt%, as determined by integration of the GC-FID peaks and material balances for both the recrystallization and Soxhlet extracts. This loading is typical for most plastic formulations.[1-3]

Hydrocracking sample preparation

HDPE pellets were used as received. Powdered HDPE was generated following a dissolution-recrystallization protocol similar to that which was described above. A 2 wt% solution of HDPE in toluene was prepared at 105 °C. Once all the polymer was dissolved, the solution was slowly cooled to room temperature without stirring. The powder was separated from the solvent using a rotary evaporator such that the additives present in the original HDPE were retained. The powder was then dried at 60 °C under vacuum for 18 h.

Hindered phenols represent the most popular primary antioxidants.[1] BHT contains a single phenol group, whereas the other examples, I-1010 and I-3114 (common trade names: Irganox® 1010 and Irganox® 3114, respectively), contain multiple phenol equivalents—four and three, respectively. The major difference between Irganox®-type antioxidants is the chemistry of the linkage group between phenols, i.e., alkyl esters for I-1010 and a cyclic triamide for I-3114. I-1010 is often considered a general-purpose antioxidant used for processing and imparting long-term stability,[4] and I-3114 is typically used in color-sensitive products, such as fibers.[1] Using this series of antioxidants, we probe the effects of common antioxidant chemical features (*e.g.,* phenol equivalent, size, linkage chemistry); however, we expect that other commercially prevalent antioxidants may have unique challenges with regards to chemical recycling that necessitate further investigation.

HDPE containing two concentrations of each antioxidant was used in this work. The lower concentration, 0.5 wt%, was selected to represent a typical antioxidant loading in commercial polyolefin products that undergo high processing or application temperatures.[1, 4, 5] The higher

concentration, 2 wt%, was used to exaggerate the effects of antioxidant chemistries on hydrocracking performance and may be found in certain application-specific polymer formulations (*e.g.,* adhesives, coatings).[1, 4, 5] Furthermore, the additive profile of commercial polyolefins characteristically contains multiple antioxidant chemistries along with other small-molecule additives,[1, 6] meaning that relevant plastics waste contain more total additives than just the antioxidants. Antioxidant-containing samples were prepared by first dissolving stripped HDPE powder in toluene at 105 °C under magnetic stirring, such that the polymer concentration was ~10 wt%. Once the polymer was fully dissolved, the desired mass of antioxidant was added to the solution, stirred, and allowed to fully dissolve for 10 min. The solution was then slowly cooled to room temperature. Solvent was removed using a rotary evaporator until the powder was mostly dry. The samples were then dried at 60 °C under vacuum for 18 h. The resulting powders consisted of approximately the same particle size and average molecular weight as the stripped HDPE (see data in **Figures S4, S8**).

Hydrocracking experiments

The platinum on tungstated zirconia hydrocracking catalyst ($Pt/WO_3/ZrO_2$) was prepared according to our previously published protocol.[7] For all reactions in this work, the catalyst contained 1 wt% Pt and 25 wt% WO_3 on the ZrO_2 support. Before the reaction, catalyst was reduced under flowing 50% H_2/He at 250 °C for 2 h (ramp rate 10 °C/min). Deconstruction of the HDPE samples was performed using 50 mL stainless steel batch pressure reactors (Parr). Polymer (2 g) was added with a desired mass (50-200 mg) of freshly reduced $Pt/WO_3/ZrO_2$ catalyst. The mixture was stirred using a magnetic stir bar to distribute the catalyst throughout the polymer. The reactor was sealed, purged with H_2 four times, and pressurized with H_2 to 30 bar (at room temperature). Then, the reactor was heated using an external band heater to 250 °C, with stirring started (at 500 RPM) when 140 °C had been reached. After 2 h reaction time, the reactor was quenched in an ice bath immediately, and the products were collected once the reaction components were below room temperature.

Hydrocracking product analysis

Gaseous products were sampled from the reactor headspace using 1 L Tedlar bags and analyzed using GC-FID (Agilent CP-Volamine GC column). Liquid and solid products were mixed with ~20 mL of DCM containing 20 mg of *n*-octacosane (C_{28}) as an internal standard. The catalyst and solid residue were filtered from the product solution (GE Whatman, 11 µm). The liquid (and DCM soluble) products were quantified using GC-FID (Agilent HP-1 column) and further identification of compounds was achieved with GC-MS (Agilent DB-1 column).[7] Retention times and response factors were calibrated via injection of a standard solution of hydrocarbons between C_1 and C_{35}.

Individual compounds were lumped by carbon number and quantified for the gaseous and liquid products (together referred to as extractable products) using the peak areas of GC-FID chromatograms, which were calculated using the response factors and peak area for the internal standard.[7] Molar yield (y_i) and selectivity (s_i) of individual extractable products were calculated as:

$$y_i = \frac{n_i}{N_0} \quad \text{(S1)}$$

$$s_i = \frac{y_i}{Y_{ex}} \quad \text{(S2)}$$

wherein n_i is the number of moles of carbon in the product group of carbon number i, N_0 is the total number of moles of carbon in the input polymer, and Y_{ex} is the overall extractable product yield (*i.e.,* the sum of all y_i).

Overall solid yields (Y_s) were determined gravimetrically by:

$$Y_s = \frac{m_s}{m_0} \tag{S3}$$

wherein m_s is the post-reaction mass of solid residue, and m_0 is the initial mass of polymer.

High-temperature gel permeation chromatography (HT-GPC)

Solid residues (including both products and unreacted HDPE) were examined using HT-GPC (Tosoh HLC-8312GPC/HT). Aliquots of the filtered residues from experiments with significant solid yields were separated from the catalyst by dissolution in toluene at 105 °C. The clear polymer solution was decanted from the catalyst particles and dried, first via rotary evaporation and then under vacuum for 16 h at 60 °C. Separated solids were reconstituted in the mobile phase (1,2,4-trichlorobenzene with 500 ppm BHT) at a concentration of 2 mg/mL and heated for at least 2 h at 140 °C. 300 µL injections of sample solutions were eluted at 0.8 mL/min at 140 °C through two TSKgel GMH_{HR}-H(20)HT columns in series, with detection via refractive index (RI) and viscometry detectors.

Molecular weight distributions were measured using the refractive index (RI) detector response. A calibration curve was constructed using runs of nine narrow polystyrene (PS) standards in the range of 6 x 10^2 g/mol to 2 x 10^6 g/mol, such that $\log M_{PS} = A_1 t_R + A_0$, wherein A_1 and A_0 are fitted coefficients, t_R is the retention time, and M_{PS} is the molecular weight with respect to PS. Molecular weights were corrected using the Mark-Houwink relationship, assuming the residues behave as model polyethylene (PE), such that:

$$\log M_{PE} = \frac{(1+\alpha_{PS})}{(1+\alpha_{PE})} \log M_{PS} + \frac{1}{(1+\alpha_{PE})} \log\left(\frac{K_{PS}}{K_{PE}}\right) \tag{S4}$$

wherein M_{PE} is the molecular weight with respect to PE (treated as the 'actual' molecular weight) and α_{PS} = 0.655 , α_{PE} = 0.725, K_{PS} = 19 µL/g, K_{PE} = 39 µL/g are Mark-Houwink constants for PS and PE in trichlorobenzene at 140 °C.[8] Yield distribution functions (*i.e.,* yields of individual components of the solid residue with the same molecular weight) were generated by:

$$y_i = Y_s \cdot H_N(t_R) = Y_s \cdot \frac{H(t_R)}{\int H(t_R) dt_R} \tag{S5}$$

wherein H_N is the normalized RI detector response calculated using the raw RI response (H) as a function of t_R, normalized by the total RI response peak area of the eluted sample. Yield distributions are displayed as a function of molecular weight (*i.e.,* a polynomial function of t_R) for evaluation; however, the total yield (Z) of a group of products within a molecular weight range must be calculated as:

$$Z = \sum_{i=j}^{k} y_i = \int_{t_R(M_k)}^{t_R(M_j)} y_i \, dt_R \tag{S6}$$

Selectivity for solid product components then can be calculated as:

$$s_i = \frac{y_i}{Y_s} = H_{N,i} \tag{S7}$$

The weight fraction distribution function (dw/d(log M)) was calculated as:[9]

$$\frac{dw}{d\log M} = \frac{-H_N(t_R)}{\left(\frac{d\log M_{PE}}{dt_R}\right)} \tag{S8}$$

wherein the divisor is the derivative of the Mark-Houwink-corrected calibration function.

The corrected selectivity value is calculated by considering the residual/unreacted HDPE signal measured as part of the HT-GPC molecular weight distribution. We define a corrected yield function:

$$Z(g)^{corr} = Z(g)^{meas} - Z(VI)^{meas}\left[\frac{Z(g)}{Z(VI)}\right]^{prist} \tag{S9}$$

wherein Z(g) is the total yield of products in group *g* and is calculated using (**S6**). The superscripts corr, meas, and prist indicate corrected yield, measured yield, and pristine HDPE values (assuming 100% solid 'yield'), respectively. Corrected selectivities of solid products are then calculated as:

$$s(g) = \frac{Z(g)^{corr}}{Z(III)^{corr} + Z(IV)^{corr} + Z(V)^{corr}} \tag{S10}$$

The forms of (**S9-S10**) are a simplified estimate of the amount of unreacted polymer; however, this analysis assumes the underlying distribution of unreacted polymer is completely unchanged and is scaled by a new concentration. Although this approach may be an oversimplification regarding the hydrocracking mechanism, it is likely to give a sufficient quantification of unreacted polymer that results in pockets of HDPE that do not diffuse to the catalyst surface or mix with hydrocracking products, and thus, reflect the starting distribution. Work in progress will provide a more sophisticated calculation method for this purpose.

For **Figures 3** and **S12**, the total product distribution was constructed by the conversion of carbon numbers (i) to M by the relationship: M = 14.027*i*. For the range of M wherein GC-FID and HT-GPC spectra overlap, spline interpolation was used to sum the two yields. This approach neglects potential band broadening or shifting of HT-GPC peaks at low M values; however, unpublished results suggest that this effect only occurs for $C_{<20}$ and is minor. The fact that deconstruction products of $C_{14\text{-}30}$ can be found in both the extractable and solid products is due to the thermodynamic partitioning of these components into the alkane-DCM extraction solution, the amorphous HDPE phase, and HDPE crystals.

Differential scanning calorimetry (DSC)

DSC was performed on as-received HDPE pellets and stripped HDPE to verify the removal of additive molecules. Approximately 5 mg of samples were loaded into hermetically sealed

aluminum pans, which were tested in the DSC (Discovery DSC, *TA Instruments*). Samples were heated from room temperature to 250 °C, cooled to -50 °C, and heated to 250 °C, all at a ramp rate of 5 °C/min. Only the first cooling and second heating cycles were analyzed. Melting (T_m) and crystallization (T_c) temperatures were determined using the maximum of the measured endotherm and exotherm peaks, respectively, and crystallinity (X_c) was calculated using the crystallization enthalpy normalized by the standard enthalpy of a perfect PE crystal (289 J/g)[10].

Diffuse reflectance infrared spectroscopy (DRIFTS)

To directly probe antioxidant-catalyst interactions, $Pt/WO_3/ZrO_2$ was treated with an excess of antioxidants in the absence of polymer. 100 mg of selected antioxidant (BHT, I-3114) or analogue (phenol) were dissolved in 2.5 g of DCM. The solution was added to 100 mg of freshly reduced $Pt/WO_3/ZrO_2$, mixed with glass stir rod, and dried at room temperature. The powder was then dried under vacuum for 12 h at 50 °C.

DRIFTS measurements of pristine and contaminated catalysts were performed on a Nicolet 8700 spectrometer equipped with a liquid-nitrogen-cooled, mercury-cadmium-telluride detector. Pure $Pt/WO_3/ZrO_2$ (~10 mg) was loaded over a quartz wool plug in an *in situ,* flow DRIFTS cell (Praying Mantis, *Harrick Scientific*). The sample was flushed with pure He for 30 min and with 10% H_2 in He for 10 min at total flow rate of 30 mL/min. Then, temperature was increased to 250 °C at a rate of 10 °C/min.

Pt metal sites were probed by keeping the sample at 250 °C for 2 h in 10% H_2 in He and then cooling to 35 °C. Gas flow was then switched to pure CO and held for 10 min followed by a 10-min flush with pure He at 30 mL/min. Spectra of the CO-saturated sample were subtracted from initial spectrum of the pristine $Pt/WO_3/ZrO_2$ sample. Brønsted acid (BA) sites were analyzed using pyridine adsorption. After the initial pretreatment at 250 °C, the sample was cooled to 150 °C and kept under pure He for 30 min, followed by five consecutive injections of 1 µL of liquid pyridine introduced via a micro-syringe and injection port. Spectra of the pyridine saturated sample were subtracted from the spectrum of the pristine $Pt/WO_3/ZrO_2$ sample.

Antioxidant-treated catalyst samples were measured using the same technique. Contaminated $Pt/WO_3/ZrO_2$ samples were loaded into the DRIFTS cell and heated in flow of 10% H_2 in He to 250 °C at 10 °C/min. No reductive pre-treatment was performed, and changes to antioxidants on the surface were easily discerned. Spectra were measured at 50 °C increments between 150 °C and 250 °C, normalized, and subtracted from the spectrum of pristine $Pt/WO_3/ZrO_2$ at the equivalent temperature.

Additional results and discussion

Evaluation of catalytic performance for HDPE

To investigate the activity of $Pt/WO_3/ZrO_2$, hydrocracking experiments were performed at varied mass loadings of catalyst with a fixed weight of HDPE. As expected, the overall yield of extractable (liquid and gas) products is proportional to the amount of catalyst (**Figure S1**). At the highest amount of catalyst (1:10 mass ratio catalyst to polymer), no solid residues were obtained. Quantification of individual carbon number products was performed using GC-FID (**Figure S2a**), and solid residues were analyzed using HT-GPC (**Figure S2b**). With increased catalyst loading,

the relative yields of C_{6-7} and C_{10} products indicate a changing degree of hydrocracking. For the 1:40 loading of catalyst, C_{10} products dominate the extractable product distribution. At 1:20 loading, C_7 and C_{10} yields are equivalent; C_{6-7} yields are ~30% greater than C_{10} yields at 1:10 loading. This trend reflects that shown by the solid yields (*i.e.,* higher activity) and suggests deep cracking of intermediate products to smaller alkanes. Solid residues from higher catalyst loading experiments contain less unreacted HDPE and greater amounts of intermediate heavy alkanes (C_{14-70}). Between the 1:20 and 1:40 catalyst loadings, an underlying peak (centered around M ~ 5 x 10^3 g/mol) in the molecular weight distribution emerges that corresponds to heavy waxes, which suggests that alkanes/PEs in this range are also intermediates. These species are most prominent for higher conversions.

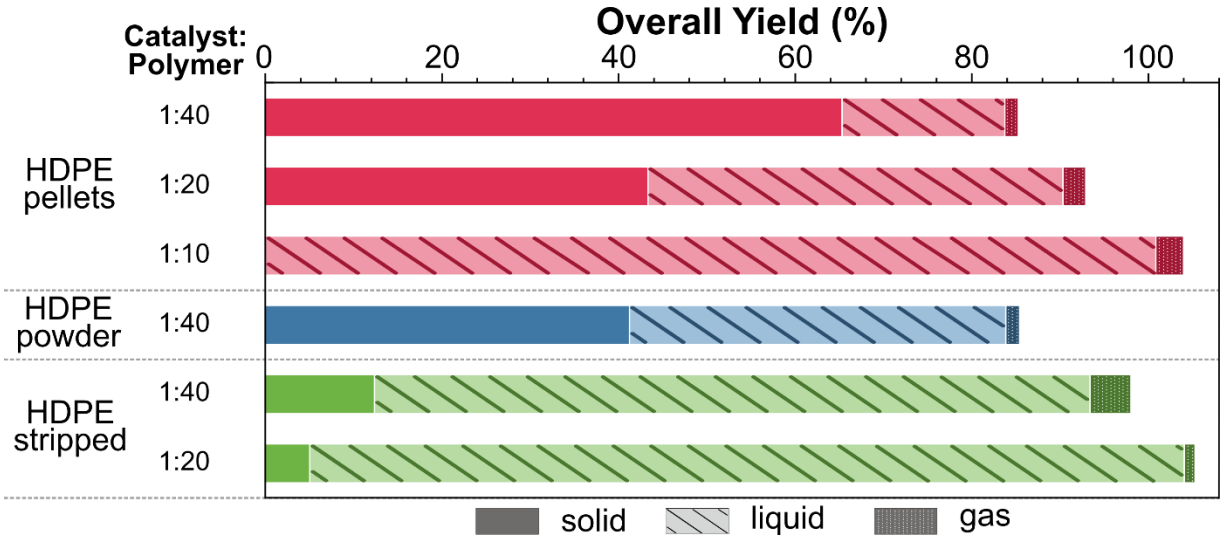

Figure S1. Overall yields of solid, liquid, and gas products for varied pristine samples with different catalyst to polymer mass ratios. Reaction conditions: 250 °C, 30 bar H_2, 2 g polymer, $Pt/WO_3/ZrO_2$, 2 h.

The mechanism by which the different populations of alkane products are generated is further understood by implementing a pseudo-Wojciechowski analysis (**Figure S3**).[11] It should be noted that for this analysis, we use extractable yield as a proxy for conversion following the example provided by previous work.[7] For carbon numbers less than 8, the product yield trend indicates stability of these products, likely because of the adhesion of polymer melt on the surface of the catalyst that excludes continued cracking of small alkanes.[7] The analysis suggests that products with carbon numbers greater than or equal to 8 are unstable (intermediate) products, due to their propensity for further cracking. Using solid product yields corrected for unreacted HDPE [via **Equations (S5), (S6),** and **(S9)**], the pseudo-Wojciechowski analysis reveals that solid products are secondary and unstable (*i.e.,* intermediates) generated by cracking of macromolecular chains.

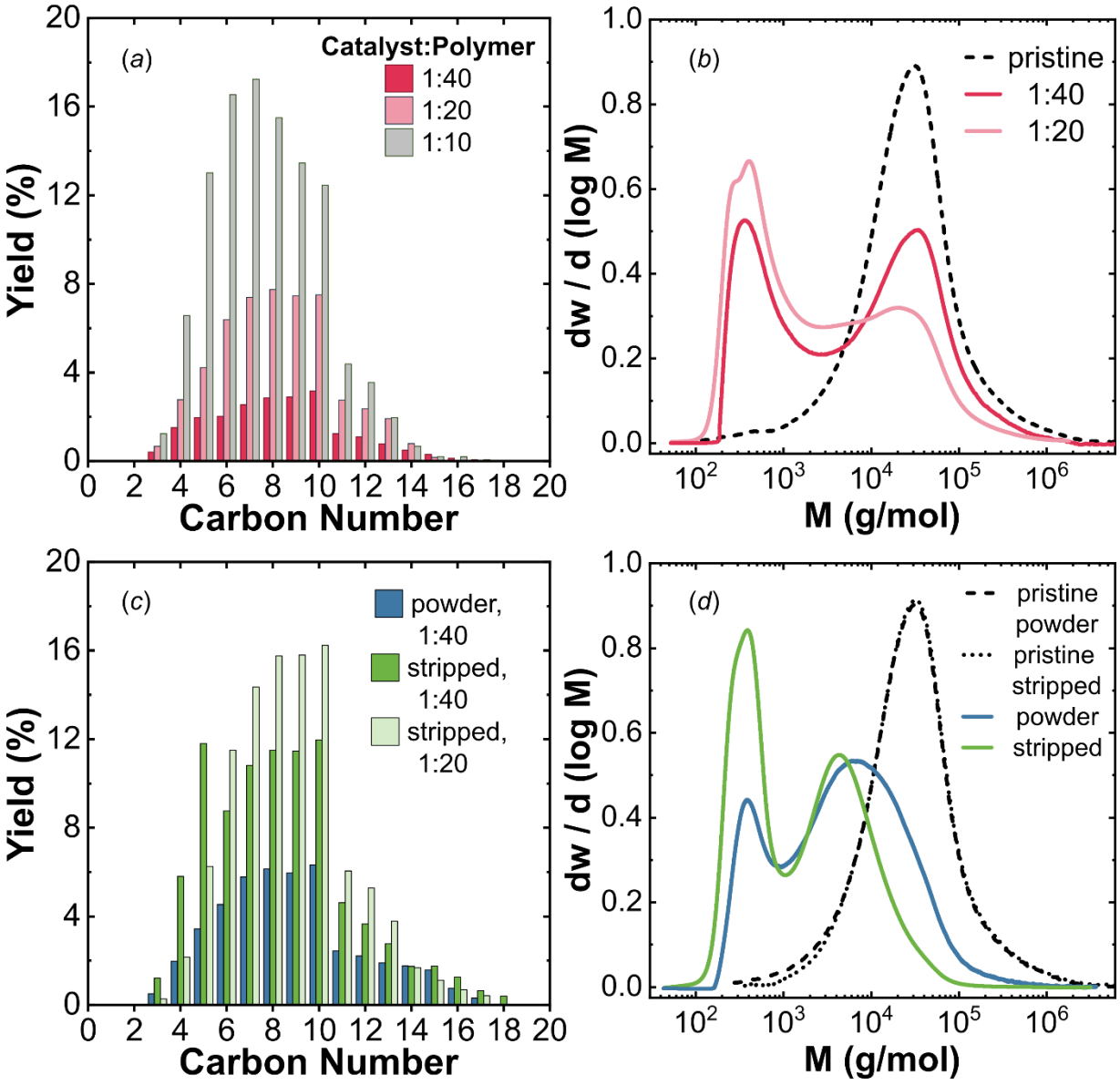

Figure S2. Extractable yield distributions from GC-FID (a,c) and molecular weight distributions from HT-GPC (b,d) for deconstruction products from HDPE samples. Results for (a-b) as-received HDPE pellets at different catalyst to polymer mass ratio and (c-d) powdered and stripped HDPE. Data in (d) are for 1:40 catalyst to polymer ratio. Dashed and dotted lines in (b,d) are molecular weight distributions of pristine input polymers. Reaction conditions: 250 °C, 30 bar H_2, 2 g HDPE, $Pt/WO_3/ZrO_2$, 2 h.

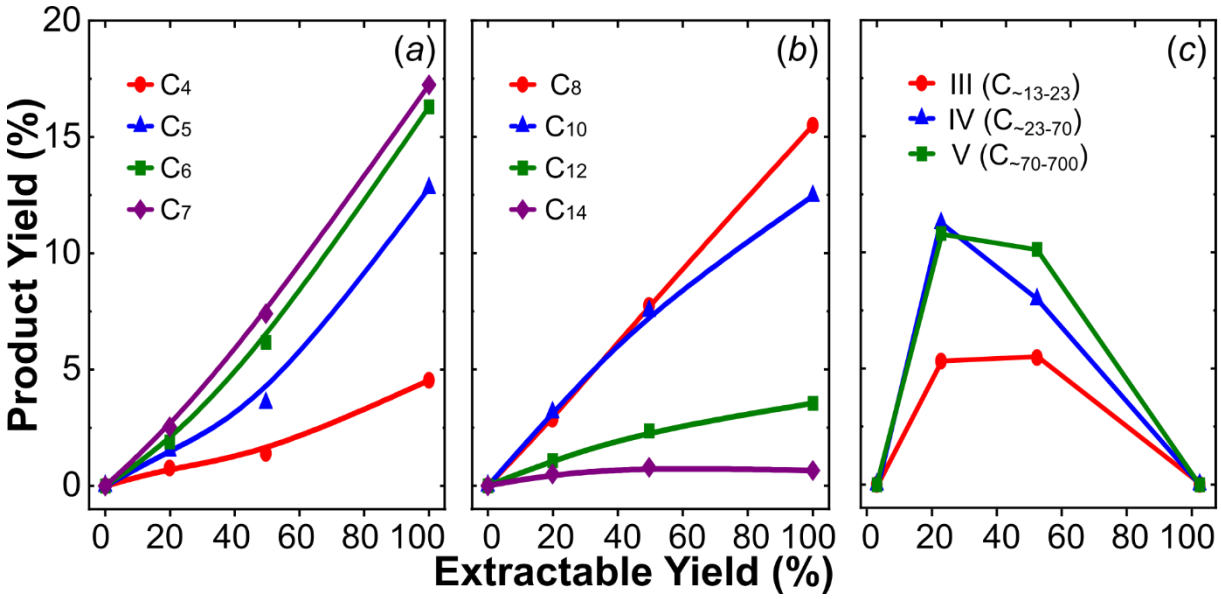

Figure S3. Pseudo-Wojciechowski analysis of product yields for HDPE pellet experiments with varied catalyst loading. Lines are drawn to guide the eye. Panels represent different product types, as defined by Ko and Wojciechowski:[11] (a) stable primary and secondary products, (b) unstable primary products, and (c) unstable primary and secondary products (in this case from the solid residue). The rightmost panel displays yields calculated from the molecular weight distribution for product types defined in Table S2 and corrected for unreacted HDPE [using **Equations (S5), (S6),** and **(S9)**]. Reaction conditions: 250 °C, 30 bar H_2, 2 g HDPE, $Pt/WO_3/ZrO_2$, 2 h.

The roles of transport phenomena (*i.e.,* form factor) and base additive profile were quantified by hydrocracking experiments performed on powdered HDPE (containing additives) and stripped HDPE (containing no additives). The overall yield of extractable products is doubled for powdered HDPE and quadrupled for stripped HDPE in comparison to the as-received HDPE pellets (**Figure S1**). This result illustrates that both distribution of the catalyst particles within the polymer melt and the absence of additive molecules enhance activity. Particle size of the starting (solid) polymer substrate is important to the distribution of catalyst particles within the polymer melt formed during heating (**Figure S4**). For pellets, catalyst particles are initially confined to small interstitial spaces and are concentrated in select areas of the melt. This configuration likely leads to a slower reaction because the amount of polymer within a single diffusion length scale of all catalyst particles is effectively smaller, but the distance between some catalyst particles is also very small. The time required to homogenize the catalyst-polymer mixture is likely significant because of the high viscosity of the polymer melt. For catalyst particles that are well-distributed prior to melting of the polymer, no mixing time is required to achieve the optimal transport of polymer to the catalyst.

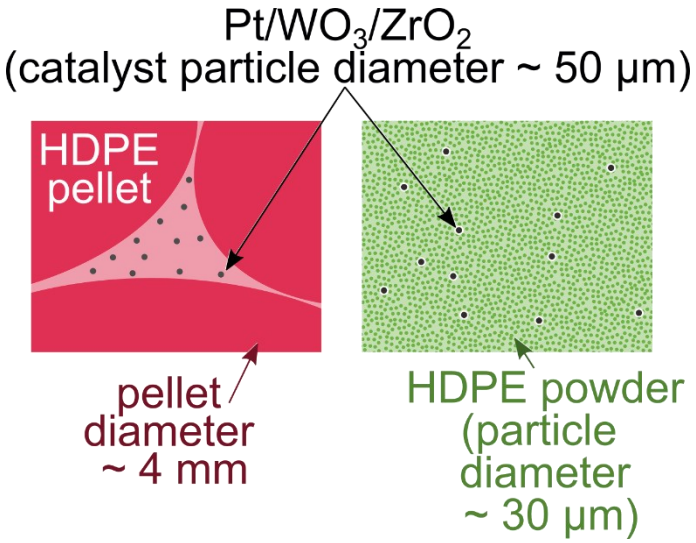

Figure S4. Illustration of the starting (room temperature) particle distribution of catalyst within HDPE for pellets (left) and powder (right), highlighting the effect of particle diameter on the amount of polymer within a single diffusion length scale of all of the catalyst.

Detailed product distributions for the hydrocracking of different form factors of HDPE and catalyst loadings reveal additional insight (**Figure S2c-d**). At equal catalyst loadings, the powder HDPE gives a similar product distribution of extractables, which validates the hypothesis that transport effects lead to lower overall yield. For stripped HDPE, the product distribution for the hydrocracking experiment at 1:40 catalyst to polymer ratio contrasts that for HDPE pellets only in the yield of $C_{4\text{-}5}$ products (**Figure S2c**), which is higher for stripped HDPE due to higher conversion that leads to deeper cracking. This effect is not seen in the distribution for stripped HDPE cracked at 1:20 catalyst loading, likely because of the higher overall conversion and the resulting narrow distribution of carbon numbers. The solid residue molecular weight distribution for the powdered HDPE exhibits peaks for the unreacted pristine polymer, a moderate molecular weight ($M \sim 3 \times 10^4$ g/mol) PE cracking product, and heavy alkanes ($M \sim 4 \times 10^2$ g/mol) (**Figure S2d**). In the case of the stripped HDPE, a significantly smaller amount of pristine HDPE remained, and a larger mass of heavy alkanes was generated, both because of higher overall conversion. This effect on the distribution highlights the mechanism by which large HDPE chains are cracked to moderate chains which are subsequently cracked to heavy alkanes before cracking to extractable range alkanes.

Quantitation of base additives in HDPE

The analysis of additives in the as-received HDPE was performed by recrystallization and Soxhlet extraction. The GC-FID chromatographs for the concentrated recrystallization extract (**Figure S5**) and Soxhlet extract (**Figure S6**) identify the presence of three major component types (neglecting impurities introduced by the extraction procedures): hydrocarbons, slip agents, and antioxidants. The alkanes and alkenes found in the extracts range from C_{12} to C_{36} and originate as oligomers and/or comonomers.[10] Each carbon number is represented by primarily normal alkanes and α-olefins, with a small amount of iso-alkanes/alkenes present. Although a distribution of hydrocarbon chain lengths is measured by GC-FID, this result is convoluted by the complex

solubility, boiling point, and participation in HDPE crystals that determine the amounts that are extracted and retained in the analyzed concentrates. The original hydrocarbon content of the HDPE is better quantified by the HT-GPC distribution, which exhibits a tail extending well into molar masses less than 10^3 g/mol for the pristine pellets that is not present in the stripped sample (**Figure S8a**). The removal of these low-molecular weight components (including the slip agents and antioxidants) increases both the crystallinity and the onset temperature for crystallization (at a given cooling rate) as shown by DSC (**Figure S8b**). This effect occurs because fewer small molecules are present to interrupt crystal formation.

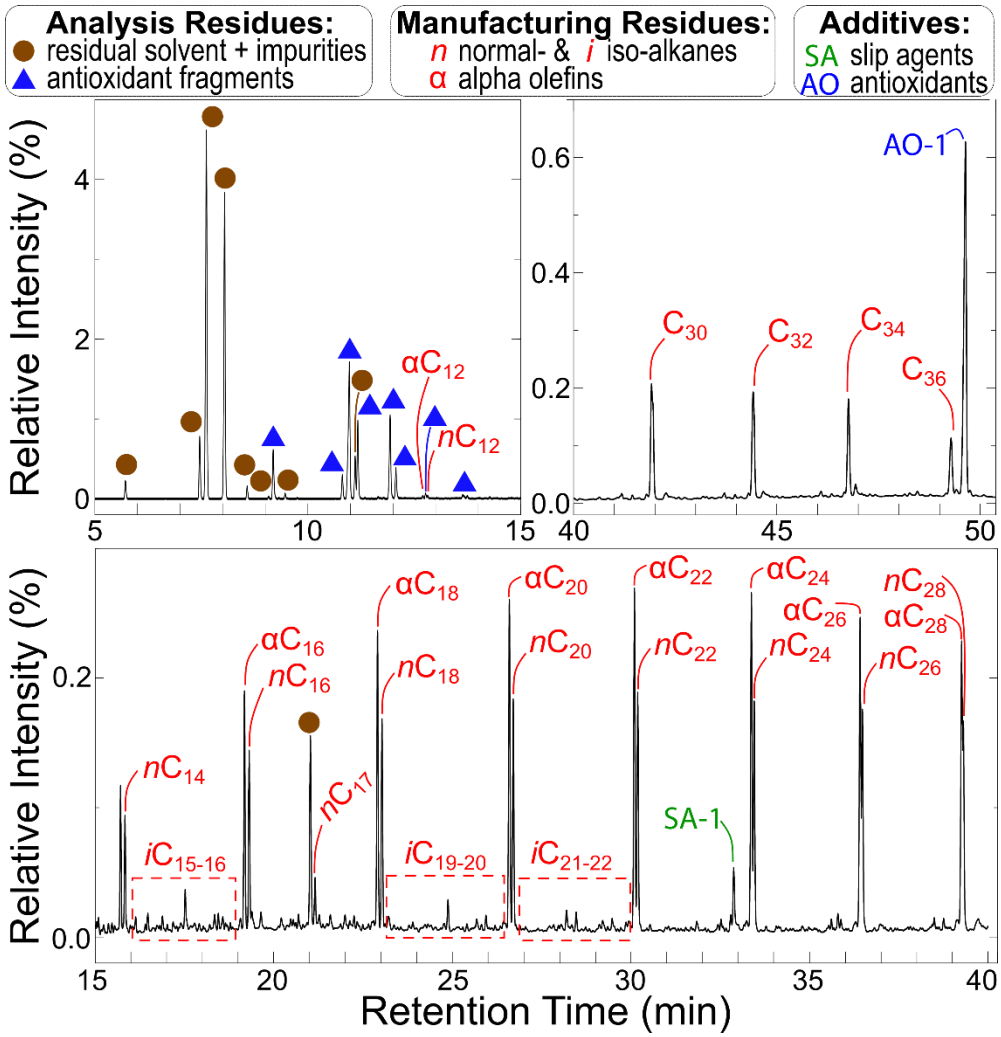

Figure S5. GC-FID chromatogram of the recrystallization extract identifying manufacturing residues and additives from the HDPE and residues generated during processing of the polymer for analysis. Note that relative intensities are defined on the basis of the chloroform (solvent) peak and retention times have been displayed out of order to emphasize the region of greatest interest. Mass spectra for slip agents and antioxidants are displayed in **Figure S7**. Compound abbreviations are defined in the legend and **Table S1.**

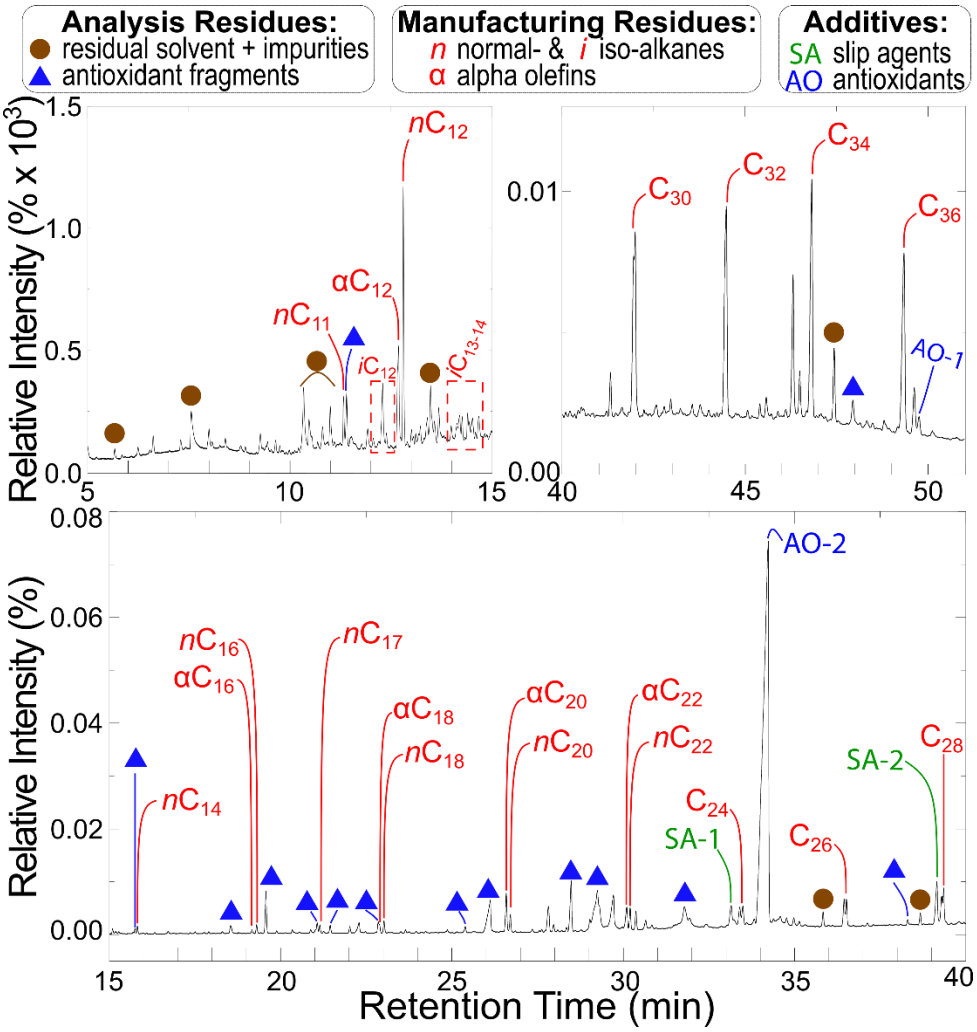

Figure S6. GC-FID chromatogram of the Soxhlet extract identifying manufacturing residues and additives from the HDPE and residues generated during processing of the polymer for analysis. Note that relative intensities are defined on the basis of the chloroform (solvent) peak. Mass spectra for slip agents and antioxidants are displayed in **Figure S7**. Compound abbreviations are defined in the legend and **Table S1.**

Two slip agents were identified in the HDPE extracts: oleamide (SA-1) and erucamide (SA-2). These fatty acid primary amides are among the most common slip agents used in commercial polyolefins and are added to reduce friction between molten plastic and extrusion equipment.[1] Two antioxidants were present in the extracted additives: an alkyl ester hindered phenol (AO-1) (common trade name: Irganox® 1076) and a di-hindered phenol (AO-2) (common trade name: Advastab® 405). Although there is a strong possibility for larger molecular weight primary and secondary antioxidants to be present in commercial HDPE,[1] further identification was not attempted. More detailed analysis of additive profiles should be considered in future works, including non-destructive quantification.[12] In addition to antioxidant molecules, fragments of antioxidants (phenolic compounds), generated by free radical degradation during processing and extraction also were found. There is a potential for these molecules to be active in poisoning of

the catalyst; however, more detailed studies would be needed to quantify the importance of this effect, as well as the involvement of large-molecule additives.

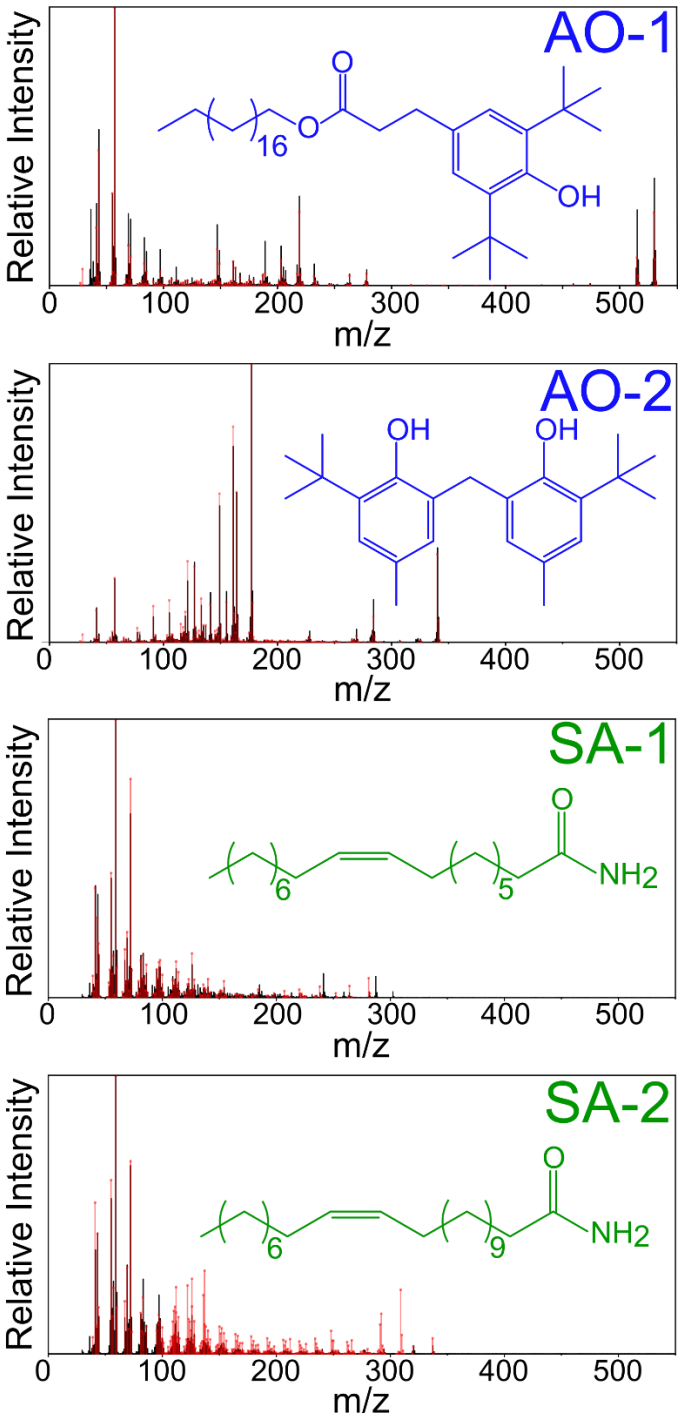

Figure S7. Measured mass spectra (black lines) and chemical structures of antioxidants found in HDPE extracts. The spectrum for AO-1 was measured from the recrystallization extract and all others from the Soxhlet extract. Red lines and points are library mass spectra for the identified compounds obtained from the NIST 2017 Mass Spectral Library.

Table S1. Summary of major chemical additives identified in GC-MS analysis of HDPE extract streams.

Class	Code	Chemical Name	Retention Time (min)
Antioxidants	**AO-1**	octadecyl 3-(3,5-di-tert-butyl-4-hydroxyphenyl)propionate	49.65
	AO-2	2,2′-methylenebis (4-methyl-6-tert-butylphenol)	34.18
Slip Agents	**SA-1**	oleamide	32.85
	SA-2	erucamide	39.12

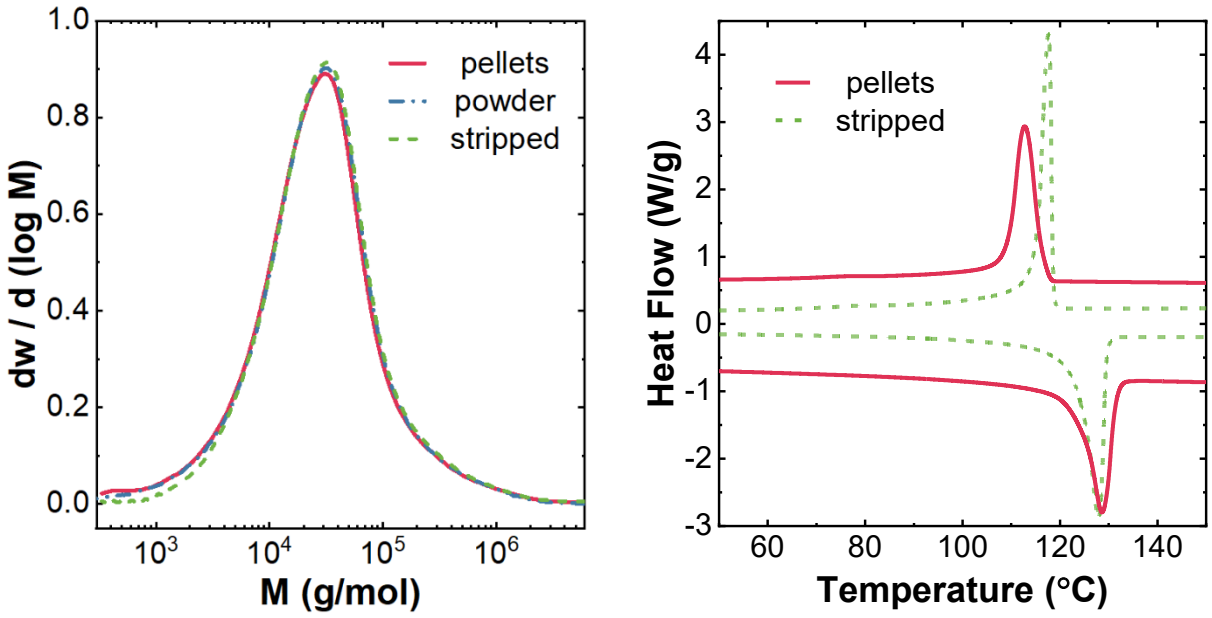

(a) (b)

Figure S8. (a) Molecular weight distribution of pristine HDPE types: as-received pellets, powdered (with additives), and stripped of additives. (b) DSC thermograms of as-received and stripped HDPE. For pellets: T_m = 128.6 °C, T_c = 112.8 °C, and X_c = 54.2%. For stripped HDPE: T_m = 128.0 °C, T_c = 117.6 °C, and X_c = 67.4%.

Evaluation of catalytic performance for antioxidant-containing HDPE

Individual product distributions were measured using GC-FID for extractables and HT-GPC for solids. The results for each antioxidant-containing sample are displayed in **Figure S9**. Note that the data for the solid residues are given as the differential weight fraction [dw/d(log M)], which is an indicator of the distribution of species within, but not the overall yield. The yields and interpretation of the results are provided in the main text. **Figure S9e** shows some small

hydrocarbons are generated for the case of 2 wt% I-3114 (and not for 0.5 wt%), likely within the batch-to-batch variability.

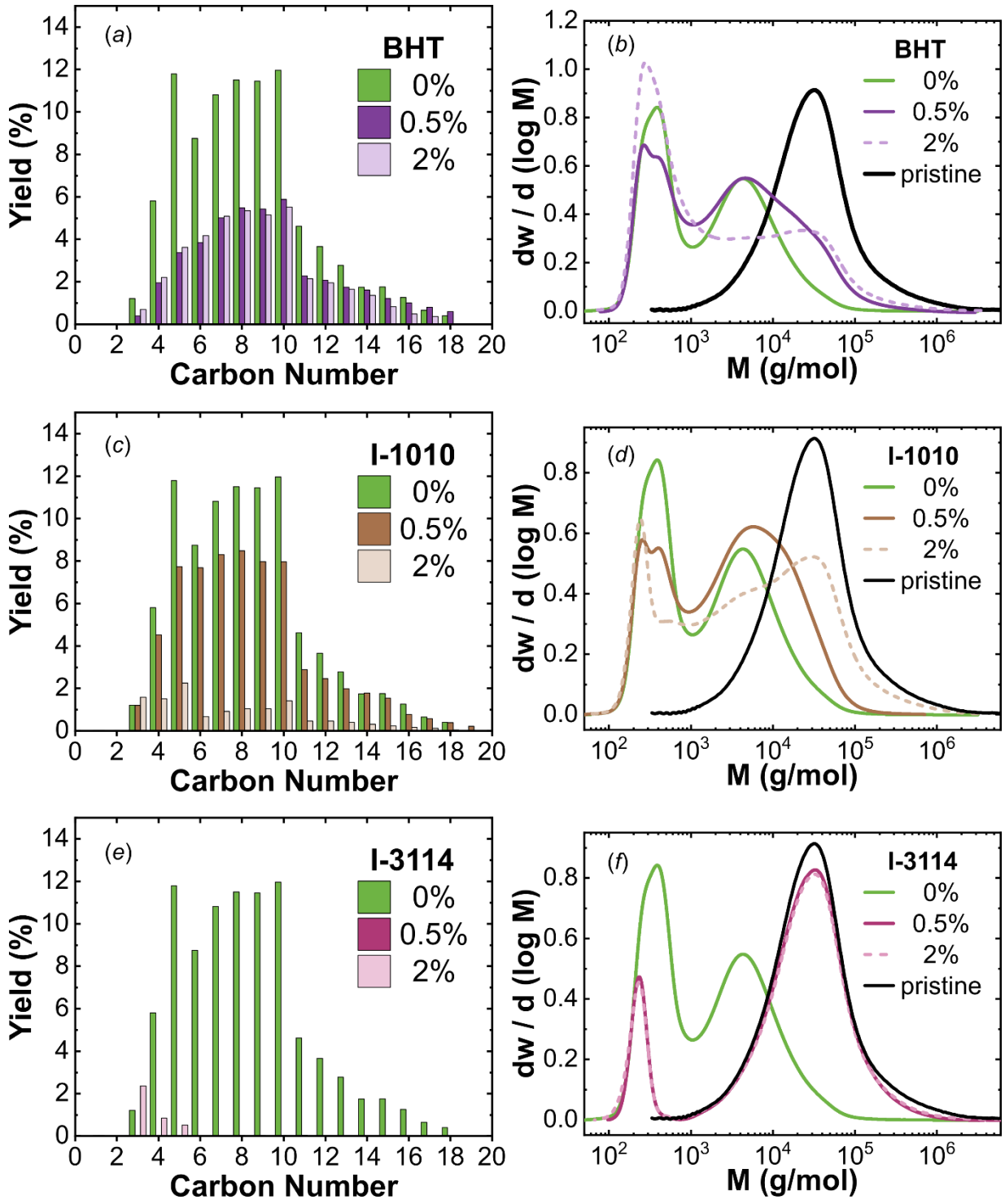

Figure S9. Extractable yield distributions from GC-FID (a,c,e) and molecular weight distributions from HT-GPC (b,d,f) for deconstruction products of antioxidant containing HDPE samples: BHT (a-b), I-1010 (c-d), and I-3114 (e-f). 0% data indicate stripped HDPE. Reaction conditions: 250 °C, 30 bar H_2, 2 g HDPE, 50 mg $Pt/WO_3/ZrO_2$, 2 h.

For convenience, the product yield distributions have been divided into regions chosen by the apparent molecular weight ranges of distinct sub-distributions that were apparent in the GC-FID and HT-GPC results (**Table S2**). The molecular weight ranges were chosen to approximate common product alkane and PE types with various molecular weights.

Table S2. Definition of product groups used in several analyses in this work.

Product Group	Log (Molar Mass) Lower Bound	Log (Molar Mass) Upper Bound	Approx. Carbon Number Range	Typical Product Uses
I	1.20	2.02	1 – 8	light fuels
II	2.02	2.25	8 – 13	
III	2.25	2.5	13 – 23	diesel fuels
IV	2.5	3	23 – 70	fuel and lubricating oils
V	3	4	70 – 700	heavy waxes, additives
VI	4	6.5	700 – $2x10^5$	commercial plastics

Product selectivities were calculated to further highlight the differences in product generation influenced by the presence of antioxidants (**Figure S10**). From this representation, quantification of product groups as a function of antioxidant-induced poisoning is possible; however, these experiments represent different catalyst activities and conversion. The effect of conversion (via changing catalyst to polymer ratio) assists comparison (**Figure S11**). For both BHT and I-1010 containing samples, the highest selectivities are toward group V and group I products for 0.5 wt% and 2 wt% antioxidant, respectively. This trend indicates deep cracking of products over more poisoned catalysts, potentially because activity for cracking of HDPE chains, but not alkanes, is diminished. For I-3114, selectivity was greatest toward group III and I for 0.5 wt% and 2 wt%, respectively This trend is similar to that for the selectivities of the other antioxidant-poisoned catalysts, but because poisoning occurs more rapidly and severely, insufficient generation of group V products occurs in favor of group III products.

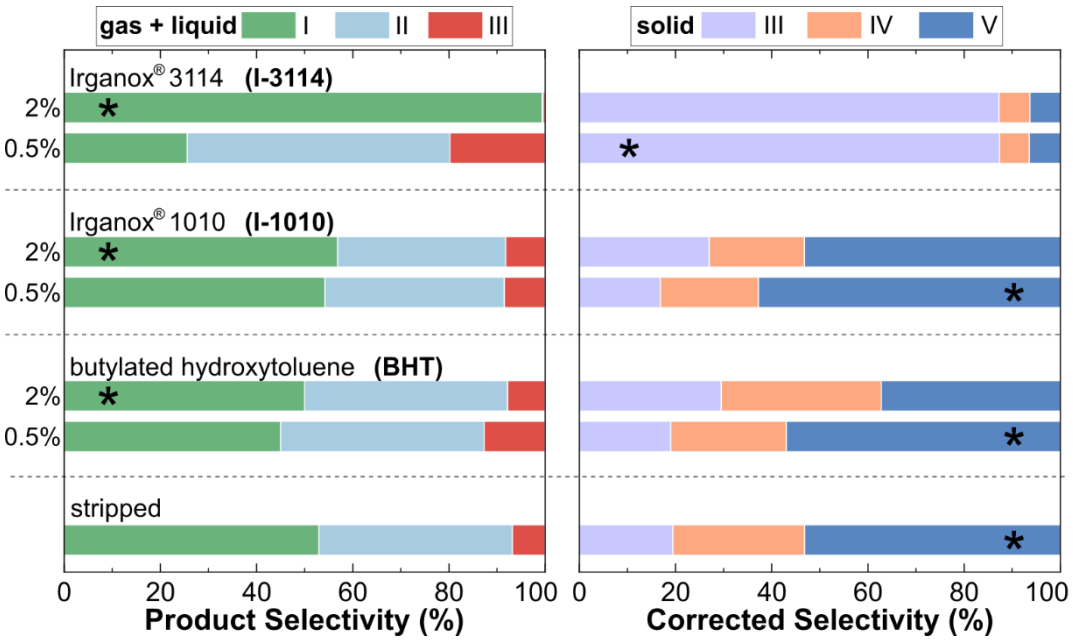

Figure S10. Selectivities of product groups (defined in Table S2) for hydrocracking of antioxidant containing and stripped HDPE. Results are from extractable products (left) and solids (right). The solid selectivities are corrected for unreacted HDPE. Asterisks indicate the highest selectivity group for each sample. Group numbers are defined in Table S2. Note that group III products obtained in the liquid and solid residues are quantified separately. Reaction conditions: 250 °C, 30 bar H_2, 2 g HDPE, 50 mg $Pt/WO_3/ZrO_2$, 2 h.

The product selectivities for hydrocracking of the base HDPE further demonstrate the effects of transport on activity. With increasing catalyst loading, the selectivity toward group V products increases because of greater conversion of HDPE. For the powdered HDPE, a greater group V selectivity was measured without significant changes to groups I, II, or III. These values indicate that the effective catalyst loading for pellets to achieve the same selectivity would be between 1:20 and 1:10 catalyst to polymer. In the case of stripped HDPE, the differences in selectivity are mainly among group III and IV products, demonstrating that the removal of additives not only improves activity but also affects the molar ratio of metal to acid sites (*i.e.*, metal-acid balance, MAB), and thus, the hydrocracking mechanism and product distribution.

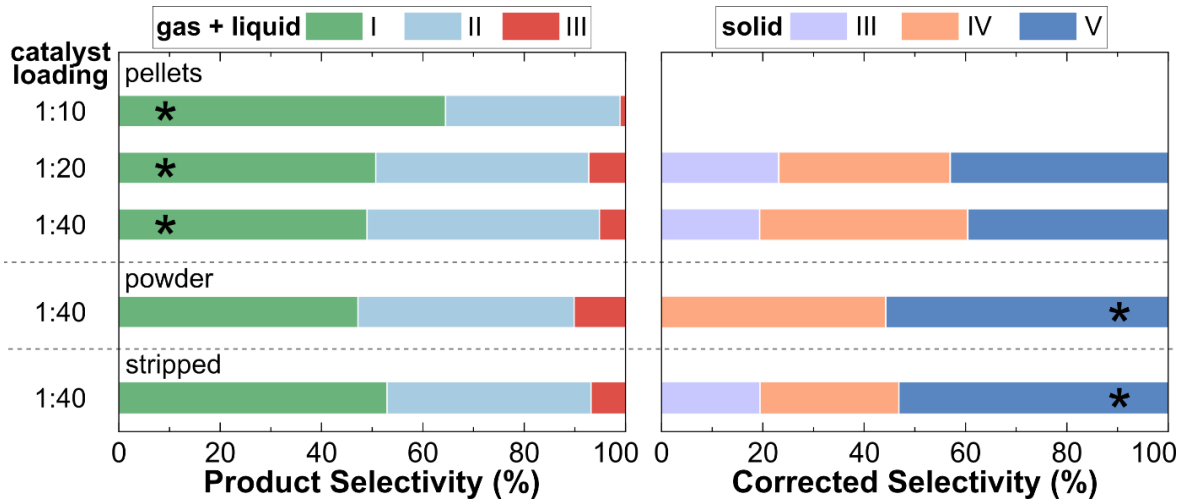

Figure S11. Selectivities of product groups (defined in Table S2) for hydrocracking of HDPE pellets, powder, and stripped powder at varying catalyst ratios (mass catalyst to mass polymer). Results are from extractable products (left) and solids (right). The solid selectivities are corrected for unreacted HDPE. Asterisks indicate the highest selectivity group for each sample. Hydrocracking of HDPE pellets at 1:10 catalyst loading yielded 0% solids therefore, selectivity cannot be calculated. Note that group III products obtained in the liquid and solid residues are quantified separately. Reaction conditions: 250 °C, 30 bar H_2, 2 g HDPE, $Pt/WO_3/ZrO_2$, 2 h.

The overall product distribution for I-3114 (**Figure S12b**) containing samples was excluded from the main text for clarity. From this distribution, it is apparent that the residues from hydrocracking are primarily unreacted HDPE. A small amount of group III products is generated at the beginning of the reaction, and for 2 wt% I-3114, a small amount of group I products is formed, likely because of further cracking of the group III products. A more detailed discussion is provided in the main text.

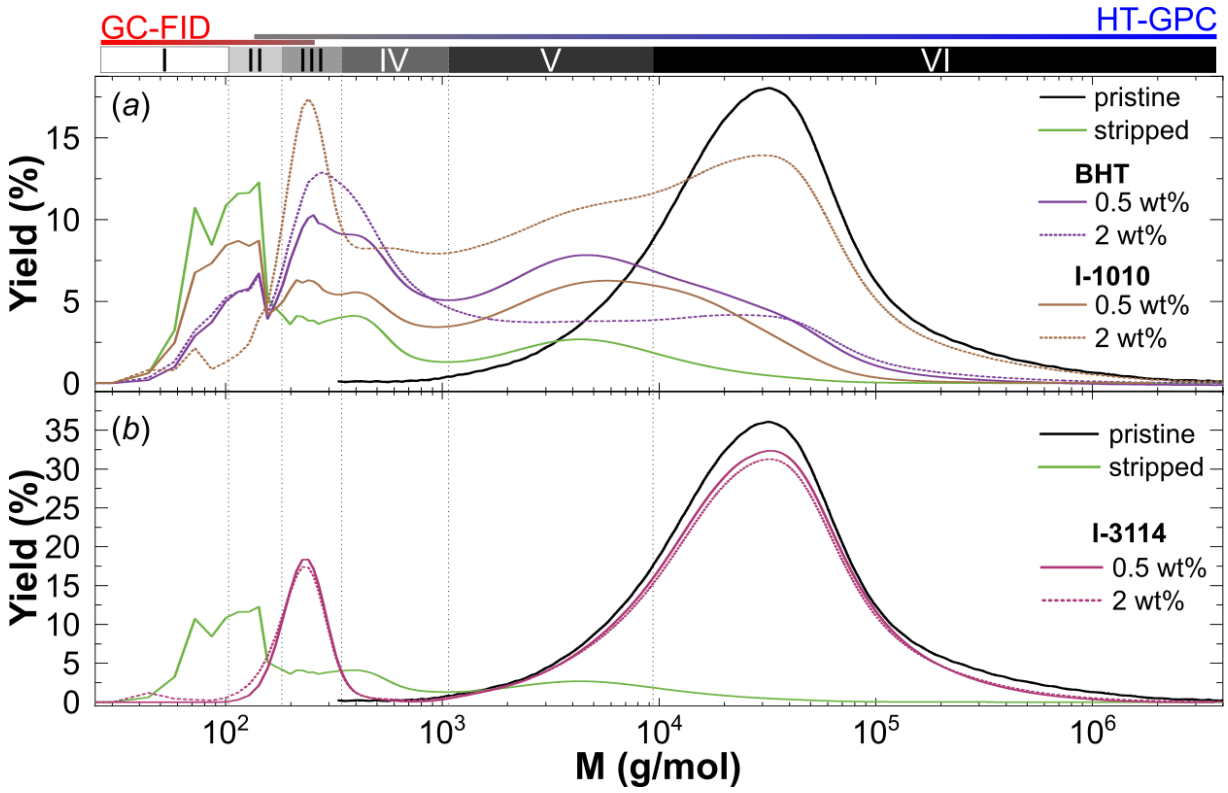

Figure S12. Product yield distribution BHT, I-1010, (a) and I-3114 (b) containing samples including pristine [arbitrarily shifted to a solid yield of 50% and 100%, respectively, in (*a*) and (*b*)] and stripped HDPE. Boxes represent approximate population ranges for: (I) light alkanes, < C_7 (II) alkanes, < C_{12} (III) mid-alkanes, < C_{24} (IV) wax, < C_{75} (V) low-molecular-weight polymer, < C_{700} (VI) high-molecular-weight polymer. Data for M < 400 g/mol are sums of the yields for extractable products (obtained from GC-FID) and solid products (obtained from HT-GPC) of approximately the same molecular weight. Typical ranges for M measured by both techniques are illustrated. Reaction conditions: 250 °C, 30 bar H_2, 2 g HDPE, 50 mg $Pt/WO_3/ZrO_2$, 2 h.

Quantification of solid residue components

HT-GPC-measured molecular weight distributions have repeatedly revealed the complexity of solid, hydrocracking residues in this and a previous work.[7] Although often considered as a proxy for activity, the overall solid yield is an insufficient indicator of selectivity because solids are only defined at room temperature and thus, contain both unreacted polymer and moderate-molecular-weight products. For this work, integration of the HT-GPC trace (**Equation S9**) was used to quantify the weight fraction of unreacted HDPE [i.e., $Z(VI)^{meas} / Y_s$] and solid products [*i.e.,* 1 - $Z(VI)^{meas} / Y_s$] (**Figure S13b,c**). The relationship between Y_s and the yield of unreacted HDPE [$Z(VI)^{meas}$] is nonlinear but monotonic. With either significant poisoning or high conversion, the yield of solid products is unsurprisingly deceased; however, the selectivities toward certain product molecular weights (discussed above) are more descriptive of the effects of poisoning.

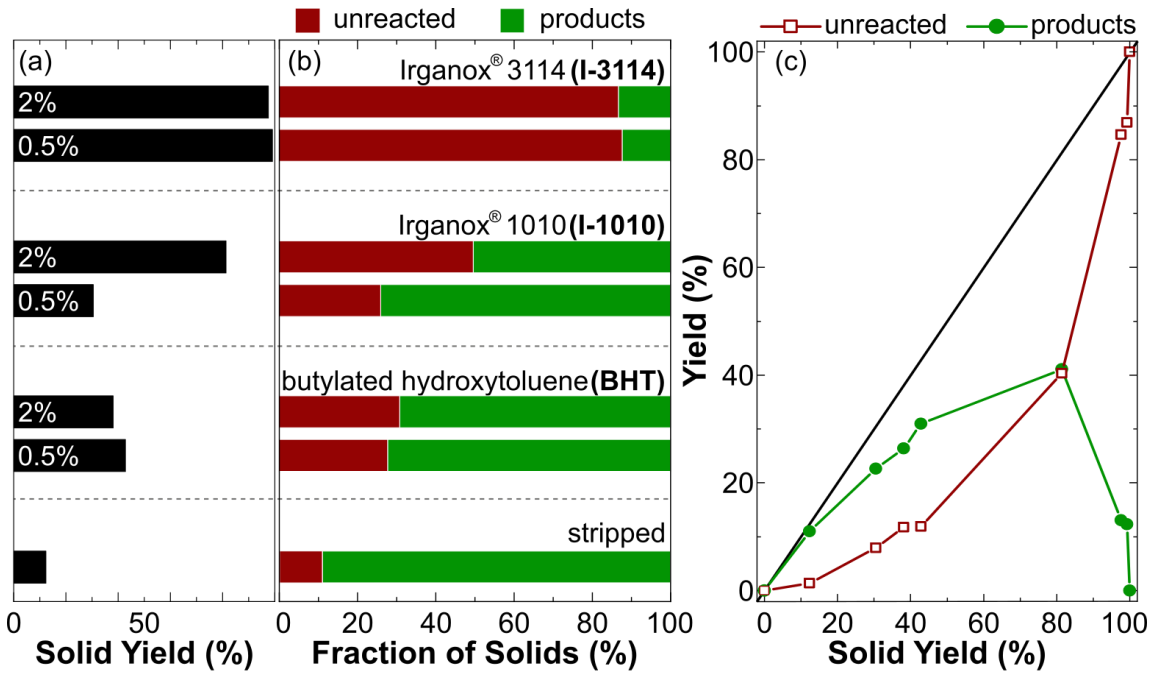

Figure S13. Analysis of solid residues of antioxidant-containing and stripped HDPE: (a) overall solid yield, (b) weight fraction of solids containing unreacted HDPE and solid products, and (c) relationship between solid product yield and overall solid yield. Reaction conditions: 250 °C, 30 bar H_2, 2 g HDPE, 50 mg $Pt/WO_3/ZrO_2$, 2 h.

The same analysis was applied to the solid residues from hydrocracking experiments of different HDPE form factors and catalyst loadings (**Figure S14**). The results from powdered HDPE and HDPE pellets at 1:40 catalyst loading demonstrate that equivalent solid yields can occur with very different solid residue compositions. Higher conversion can occur at a short length scale because of transport effects, such that continued scission of C-C bonds occurs for only a select population of PE/alkanes, while another population of HDPE remains unreactive. The scaling of diffusion rate with alkane/PE molecular weight (*i.e.,* larger molecules diffuse more slowly) likely means that smaller alkane products can further react (because of their proximity to the catalyst) over the time that it takes HDPE to diffuse toward the catalyst surface. This difference would lead to more turnovers for one population of molecules (those that first reacted) and no reaction for a population of undiluted HDPE (that could not diffuse over sufficient length scales during the reaction time). Therefore, there is likely an induction time to achieve a pseudo-steady state, with the product distribution being a complex function of time. Additional studies of transport phenomena in deconstruction systems are ongoing.

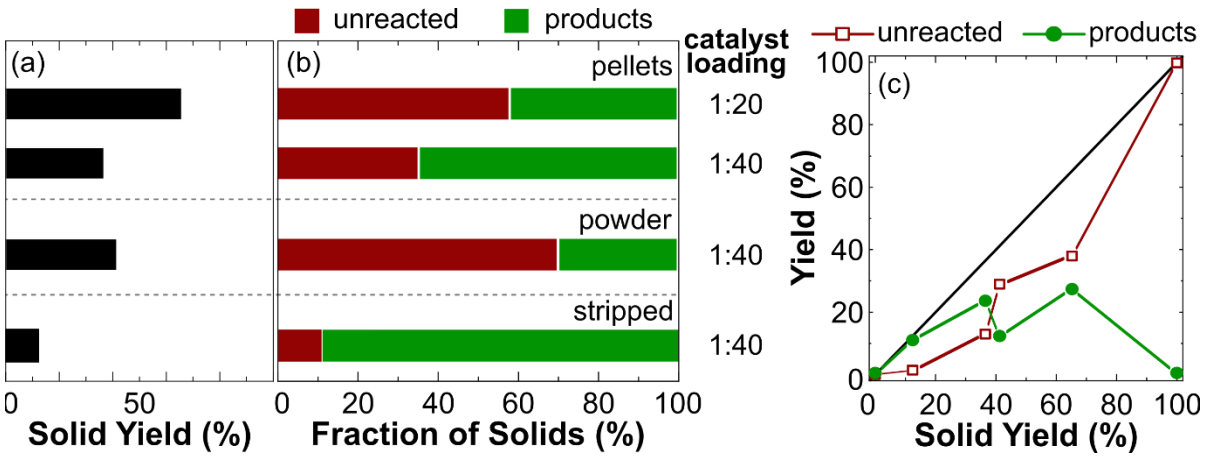

Figure S14. Analysis of solid residues of pellets, powders, and stripped HDPE at different catalyst loadings: (a) overall solid yield, (b) weight fraction of solids containing unreacted HDPE and solid products, and (c) relationship between solid product yield and overall solid yield. Reaction conditions: 250 °C, 30 bar H_2, 2 g HDPE, $Pt/WO_3/ZrO_2$, 2 h.

Identification of catalyst-antioxidant interactions

Infrared spectroscopy studies of catalyst-antioxidant interactions were performed to elucidate the differences in poisoning from different chemistries. Metal and acid sites of the catalyst were individually probed using CO and pyridine adsorption, respectively. Additional experiments examining antioxidant- or antioxidant analog-treated catalysts were performed using DRIFTS to quantify the molecular changes that occur after poisoning. Phenol was selected to quantify the potential reactions common to all of the phenolic antioxidants used in this work. Adsorption of phenol to $Pt/WO_3/ZrO_2$ completely eliminates the band corresponding to free, unperturbed hydroxyls (3630 cm^{-1}) contributed by BA sites (**Figure S15**). A new band appears corresponding to hydrogen-bonded hydroxyls (3530 cm^{-1}) together with a C-H stretching vibration of the phenol ring (~3065 cm^{-1}). These features indicate the presence of adsorbed phenol. Additionally, new peaks in the 2970-2850 cm^{-1} region arise due to the formation of aliphatic C-H groups (methyl and methylene). This change in the spectrum suggests that the aromatic ring of phenol undergoes hydrogenation to cyclohexanol during the treatment stage (*i.e.,* near hydrocracking conditions), following the proposed scheme in **Figure S16a**. Multiple bands due to the double bond in an aromatic ring appear at 1603, 1583, 1497 and 1450 cm^{-1}, corresponding to phenol but shifted from those peaks measured for liquid phenol, and a broad band at 1450 cm^{-1} is contributed by a CH_2 bend of cyclohexanol. Cyclohexanol can easily dehydrate over BA sites to form cyclohexene (**Figure S16a**) via an intermediate adsorbed phenol or phenoxy species, which contributes to the strong vibration of C-O at 1280-1261 cm^{-1}.[13] From this proposed mechanism, we expect phenol-mediated poisoning to be reversible and generate additional product species. Therefore, the number of hindered phenol groups within the structure of an antioxidant is not as significant a parameter as the number or type of other functional groups, such as esters or acids.

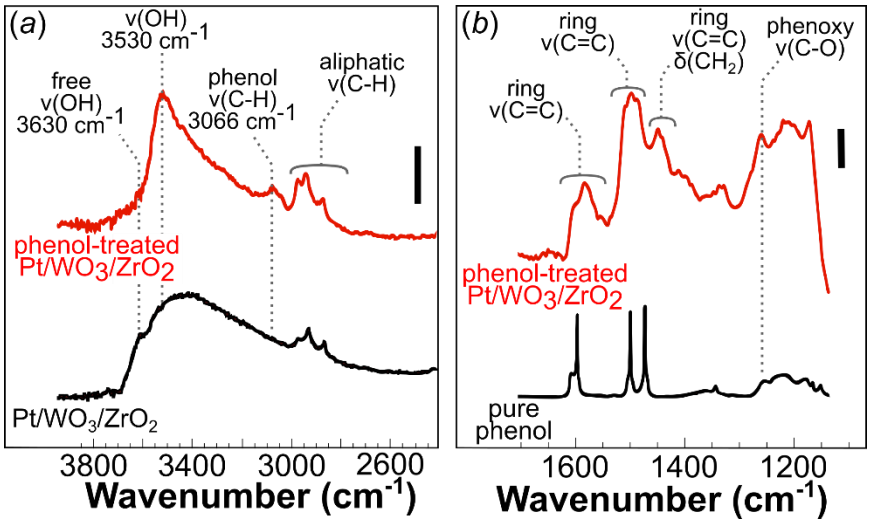

Figure S15. DRIFTS traces of pristine and phenol-treated $Pt/WO_3/ZrO_2$ and pure phenol measured at 250 °C: (a) O-H and C-H bond-stretching region and (b) deformation vibration region. Scale bars indicate identical (arbitrary) absorbance units. *v* and δ indicate a stretching or bending vibration, respectively.

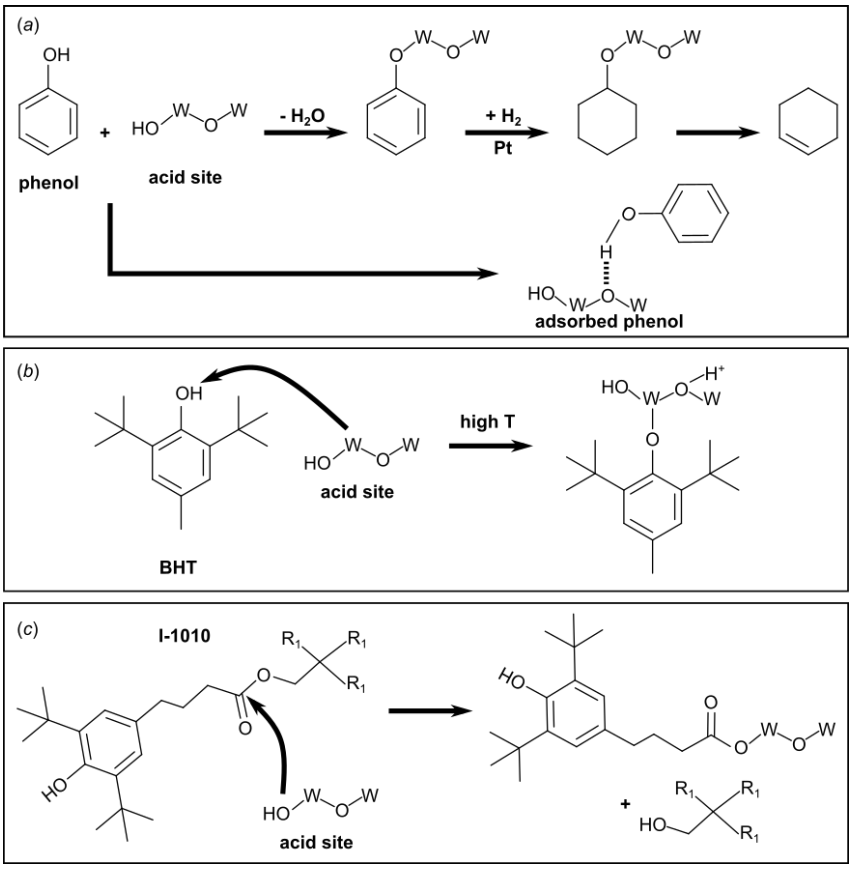

Figure S16. Proposed reaction schemes of antioxidant-mediated catalyst poisoning: (a) The adsorption or reaction of phenol to form phenoxy species and cyclohexene over acid sites, (b) bridge formation between BHT and acid sites at high temperature, and (c) the reaction of ester carbons in I-1010 to form acid-site complexes.

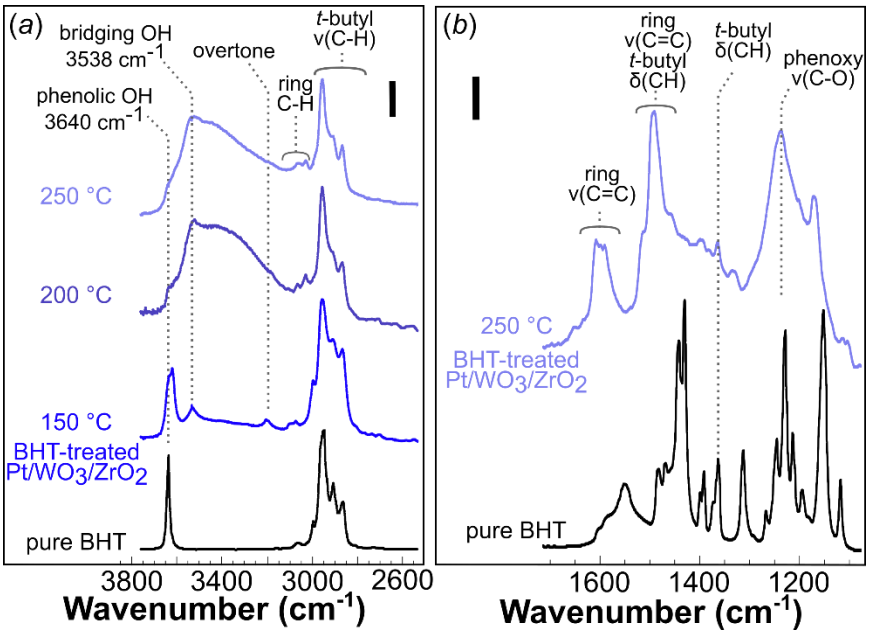

Figure S17. DRIFTS traces of BHT-treated $Pt/WO_3/ZrO_2$: a) O-H and C-H bond-stretching region at different pretreatment temperatures and b) deformation vibration region of pure BHT and treated catalyst after 250 °C pretreatment. Sample pretreatment: for (a) 10% H_2/He flow, heating rate 10 °C/min; for (b) 250 °C, 2 h, 10% H_2/He flow.

DRIFTS traces for BHT-treated $Pt/WO_3/ZrO_2$ reveal interactions of BHT with the catalyst similar to those seen for phenol. In this case, temperature dependent spectra were captured to further highlight the poisoning mechanism (**Figure S17**). At low temperatures (<150 °C), BHT does not react, particularly because of the stability of the C-O bond induced by the steric hinderance of *t*-Bu groups. Free -OH groups of BHT contribute to the spectra via stretching vibrations at 3640 and 3622 cm^{-1}, and the C-H stretching region reflects that for liquid BHT including: 3076 cm^{-1} from aromatic C-H stretching, 3000 cm^{-1} from asymmetric CH_3 stretching, and peaks at 2960-2867 cm^{-1} from *t*-Bu groups. At higher temperatures, BHT reacts with the catalyst surface and forms phenoxy species and products of ring hydrogenation, similar to the phenol case. A new peak at 3538 cm^{-1} emerges due to the bridging -OH group formed according to the scheme in **Figure S16b**. The methyl group peak is no longer separable from *t*-Bu signals and a set of broad peaks appear at 1609 and 1493 cm^{-1} caused by aromatic ring vibrations and bending of *t*-Bu groups. A strong peak at 1240 cm^{-1} emerges because of C-O vibrations from phenoxy species. These data suggest that poisoning via phenoxy formation is the cause of BHT-induced poisoning; however, the shielding of this bond by *t*-Bu groups may lead to lower degrees of catalyst-antioxidant interactions.

Aside from a higher phenol content, I-1010 has a higher propensity for catalyst poisoning because of the presence of ester bridging groups. Because the ester linkage is prone to hydrolysis at elevated temperatures,[14] interactions between acid sites I-1010 or fragments of I-1010 have more potential for poisoning (*e.g.,* via the proposed reaction pathway in **Figure S16c**) than the phenol groups alone. For the antioxidant that exhibited the most severe poisoning, I-3114, it stands to reason that the central cyanuric acid functional group also plays a key role in consumption of acid sites.

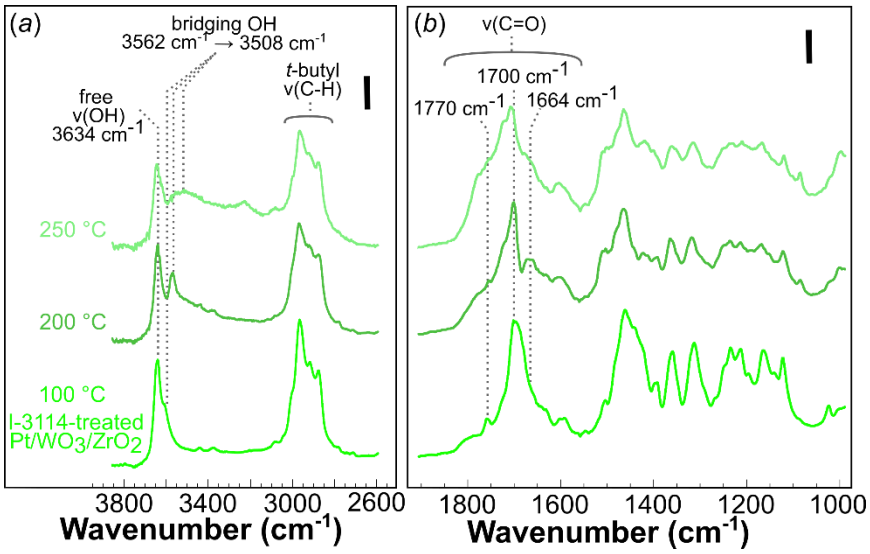

Figure S18. DRIFTS traces of $Pt/WO_3/ZrO_2$ catalyst treated with I-3114 at different temperatures. Sample pretreatment: 10% H_2/He flow, heating rate 10 °C/min.

DRIFTS traces highlight the temperature dependent effect of I-3114 on $Pt/WO_3/ZrO_2$ (**Figure S18**). At low temperature, I-3114 does not interact with the catalyst. Free -OH groups are indicated by the stretching vibration that appears at 3634 cm^{-1}. Peaks of *t*-Bu groups appear in the region of 3000-2875 cm^{-1}. Low-wavenumber peaks exhibit the same set of bands as pure I-3114.[14] As temperature is increased, new peaks arise at 3562 cm^{-1} due to formation of bridging hydroxyls similar to the case of BHT (**Figure S17**). At higher temperatures, this peak shifts even further to 3508 cm^{-1}, but some residual signal of free, unperturbed I-3114 remains, even at 250 °C. This result suggests that binding with WO_3/ZrO_2 sites at phenolic -OH groups is sterically hindered, to some degree, by *t*-Bu groups. Cyanuric acid residues in central functional group of I-3114 likely will interact with BA sites more strongly in comparison to the -OH groups at the periphery of the molecule. This hypothesis is further supported by spectra in the low-wavenumber region (**Figure S18b**). The major peak of the C=O group in the amide fragment of the cyanuric acid residue shifts from its original value of 1700 cm^{-1} to 1770 cm^{-1} and 1664 cm^{-1}. This shift suggests that the amide group is involved in interactions with BA sites of the catalyst at T > 250 °C. Decomposition of pure cyanuric acid is known to form urea, biuret (urea dimer), or isocyanic acid,[15] thus these compounds are a potential source of poisoning from I-3114. Formation of these products shifts the C-O vibration from its initial position at 1700 cm^{-1}. The majority of other bands in the 1530-1070 cm^{-1} range correspond to the initial I-3114, likely due to the low quantity required for complete poisoning of the catalyst. These experiments highlight the need for consideration of degradation products of antioxidants during selection due to potential implications for chemical recycling.

Acknowledgements

This work was supported as part of the Center for Plastics Innovation, an Energy Frontier Research Center funded by the U.S. Department of Energy, Office of Science, Basic Energy Sciences, under award DE-SC0021166.

References

1. M. Tolinski, *Additives for Polyolefins: Getting the Most Out of Polypropylene, Polyethylene and TPO*, William Andrew, Waltham, MA, 2nd Ed. edn., 2015.
2. *Polymer Modifiers and Additives*, CRC Press, Boca Raton, FL, 2018.
3. M. Bolgar, J. Hubball, J. Groeger and S. Meronek, *Handbook for the Chemical Analysis of Plastic and Polymer Additives*, CRC Press, Boca Raton, FL, 2008.
4. BASF, *Irganox® 1010 Technical Information*, 2015, https://dispersions-resins-products.basf.us/products/irganox-1010, (accessed April 2022).
5. BASF, *Irganox® 3114 Technical Data Sheet*, 2019, https://documents.basf.com/7758655303a3460c5a14914b17d6cf15ffefc531/Irganox_3114_July_2019_R3_Adhesives.pdf, (accessed April 2022).
6. H. Wiesinger, Z. Wang and S. Hellweg, *Environ Sci Technol*, 2021, **55**, 9339.
7. B. C. Vance, P. A. Kots, C. Wang, Z. R. Hinton, C. M. Quinn, T. H. Epps, III, L. T. J. Korley and D. G. Vlachos, *Applied Catalysis B: Environmental*, 2021, **299**, 120483.
8. D6474-20, *Standard Test Method for Determining Molecular Weight Distribution and Molecular Weight Averages of Polyolefins by High Temperature Gel Permeation Chromatography*, ASTM International, West Conshohocken, PA, 2020.
9. D5296-19, *Standard Test Method for Molecular Weight Averages and Molecular Weight Distribution of Polystyrene by High Performance Size-Exclusion Chromatography*, ASTM International, West Conshohocken, PA, 2019.
10. A. J. Peacock, *Handbook of Polyethylene: Structures, Properties, and Applications*, Marcel Dekker, New York, 2000.
11. A. N. Ko and B. W. Wojciechowski, *International Journal of Chemical Kinetics*, 1983, **15**, 1249.
12. D. C. M. Squirrell, *Analyst*, 1981, **106**, 1042.
13. A. Popov, E. Kondratieva, J.-P. Gilson, L. Mariey, A. Travert and F. Maugé, *Catalysis Today*, 2011, **172**, 132.
14. Y. Wang, H. Ren, Y. Yan, S. He, S. Wu and Q. Zhao, *Polymers and Polymer Composites*, 2020, **29**, 1403.
15. A. M. Bernhard, D. Peitz, M. Elsener, A. Wokaun and O. Kröcher, *Applied Catalysis B: Environmental*, 2012, **115-116**, 129.